Rigorous and Non-Rigorous Photogrammetric Processing of Ikonos Geo Image

M. J. Valadan Zoej [1], S. Sadeghian [2]

[1] Faculty of Geodesy and Geomatics Engineering, K.N. Toosi University of Technology, No. 1346, P.O.Box 19697, Tehran, IRAN, Valadanzouj@KNTU.ac.ir

[2] Research Department of National Cartographic Centre (NCC), Tehran, IRAN, P.O.Box: 13185-1684, Sadeghian@ncc.neda.net.ir

Joint Workshop of ISPRS Working Groups I/2, I/5, IC WG II/IV, and EARSeL Special Interest Group: 3D Remote Sensing

KEY WORDS: DLT, SDLT, 3D Affine, Orbital parameter model, Ikonos Geo, Accuracy

ABSTRACT:

Although Ikonos imagery has been commercially available since early 2000, the use of this imagery and especially the scientific investigations on its potential use in various applications have been affected by various points, the main ones are related to the policy of Space Imaging and also high spatial, spectral, temporal and radiometric resolutions of Ikonos image as well as flexible viewing capability of the satellite. Geopositioning accuracy of Ikonos panchromatic Geo image is investigated in this paper. The DLT, SDLT, 3D affine and orbital parameter model been applied in tests with Ikonos Geo image. The test area considered covers Hamedan city of Iran. Taking into account the quality of the ground control, an optimal planimetric accuracy of 0.89m was achieved using an orbital parameter model.

1. INTRODUCTION

After the successful launch and deployment of Ikonos-2 satellite in September 24, 1999, EROS-A1 in December 5, 2000, QuickBird-2 in October 18, 2001, SPOT5 in May 4, 2002 and OrbView 3 in June 26, 2003, the era of commercial high resolution earth observation satellites for digital mapping had began. Successful exploitation of the high accuracy potential of these systems depends on a comprehensive mathematical modeling of the imaging sensor. An orbital parameter model can be applied to stereo space imagery in order to determine exterior orientation parameters, and a number of papers have been published on different approaches for the position and attitude determination of SPOT, IRS-1C/D, MOMS and other sensors (Gugan, 1986;Dowman, 1991;Fraser & Shao, 1996;Radhadevi et al., 1998). Unfortunately the ancillary data (position, velocity vectors and angular rates) of the satellite platform have not been provided with Ikonos imagery, therefore alternative ways of camera modeling need to be employed. Recently, several 2D and 3D approaches have been reported to tackle this issue (Sadeghian and Delavar, 2003; Dowman and Tao, 2002; Fraser et al., 2002a, 2002b; Valadan et al., 2002; Hanley and Fraser, 2001; Sadeghian et al., 2001a, 2001b; Tao and Hu, 2001, 2002). They do not require interior orientation parameters or orbit ephemeris information. The image to object space transformation solution is based only upon ground control points (GCPs). This is an advantage for processing the new high resolution satellite imagery (HRSI). In this paper the possibility of using non-rigorous and rigorous sensor models for 2D ground point determination from Ikonos Geo image is investigated.

2. IKONOS SYSTEM

Ikonos-2, has a polar sun-synchronous orbit with an inclination of 98.1º at a height of 680 km. The satellite payload consists of both a 1m panchromatic and 4-band (blue, green, red, near-infrared), 4m multispectral 11-bit sensors. Ikonos travels at a speed of 7 km/s, which allows it to orbit the planet every 98 minutes. The system is equipped with GPS receivers and digital star trackers to establish precise camera position and attitude. Details of the Ikonos satellite and its camera systems are given in Gerlach (2000) and Grodecki & Dail (2001). The Ikonos system is based on a pushbroom scanner with a lens of 10 m focal length that has been folded into a 2m length through the use of two additional flat mirrors incorporated into its telescope. This significantly reduces the physical size and weight of the camera

3. ORIENTATION MODELS

At this writing, Space Imaging has refused to release information on the sensor model for Ikonos, as well as data on the precise in-flight position and attitude of the imaging sensor. This means that a large number of photogrammetric parameters are unknown and not readily determinable from the imagery alone. The very long focal length and narrow angle of view (0.93°) and swath (~11 km) will likely make an orbital resection unstable, and even if many GCPs and several images are used, an accurate solution might not be possible. There is consequently a need for a range of alternative, practical approaches for extracting accurate 2D and 3D terrain information from HRSI. In the following discussion, DLT, SDLT and 3D affine, are evaluated as potential approximate sensor models to substitute for the rigorous physical sensor model. Also in this paper the possibility of using a rigorous model (orbital parameter modeling) for ground point determination were explored and investigated. The orbital parameters and ephemeris data have been approximated from meta data, image file and celestial mechanics. These parameters then have been used in the orbital parameter modeling.

3.1. Rational Functions

Under the model, an image coordinate is determined from a ratio of two polynomial functions, in which the image (x,y) and ground coordinates (X,Y,Z) have all been normalized (OGC, 1999):

x = P1(X,Y,Z)/P2(X,Y,Z) =

$$\sum_{i=0}^{m1}\sum_{j=0}^{m2}\sum_{k=0}^{m3} a_{ijk} X^i Y^J Z^k \Big/ \sum_{i=0}^{n1}\sum_{j=0}^{n2}\sum_{k=0}^{n3} b_{ijk} X^i Y^J Z^k$$

y = P3(X,Y,Z)/P4(X,Y,Z) =

$$\sum_{i=0}^{m1}\sum_{j=0}^{m2}\sum_{k=0}^{m3} c_{ijk} X^i Y^J Z^k \Big/ \sum_{i=0}^{n1}\sum_{j=0}^{n2}\sum_{k=0}^{n3} d_{ijk} X^i Y^J Z^k \quad (1)$$

The rational function method (RFM) maps three-dimensional ground coordinates to image space for all types of sensors, such as frame, pushbroom, whiskbroom and SAR systems. The direct linear transformation (DLT), self calibration DLT (SDLT) and 3D affine equations are specialized forms of the RFM, and we now consider these models.

3.1.1. Direct Linear Transformation (DLT)

Eleven linear orientation parameters define the relationship between 2D image space and 3D object space:

$$x = \frac{a_o + a_1X + a_2Y + a_3Z}{1 + c_1X + c_2Y + c_3Z}, \quad y = \frac{b_o + b_1X + b_2Y + b_3Z}{1 + c_1X + c_2Y + c_3Z} \quad (2)$$

3.1.2. Self Calibration Direct Linear Transformation (SDLT)

Twelve linear orientation parameters define the relationship between 2D image and 3D object space:

$$x = \frac{a_o + a_1X + a_2Y + a_3Z}{1 + c_1X + c_2Y + c_3Z} + a_4xy, \quad y = \frac{b_o + b_1X + b_2Y + b_3Z}{1 + c_1X + c_2Y + c_3Z} \quad (3)$$

3.1.3. 3D Affine Transformation

Eight parameters define the relationship between the object and image spaces:

$$x = a_o + a_1X + a_2Y + a_3Z, \quad y = b_o + b_1X + b_2Y + b_3Z \quad (4)$$

In the above functions *x,y* are the coordinates on the image; *X,Y,Z* are the coordinates on the ground; and a_i, b_i, c_i, d_i are transformation parameters.

3.2. Orbital parameter model

An orbital parameter model can be applied to the pushbroom images in order to determine their exterior orientation parameters. An orbital resection method has been developed to model continous changing of position and attitude of the sensors by finding the orbital parameters of the satellite during the period of its exposure of the image. A bundle adjustment has been developed to determine these parameters using GCPs. This program has been already tested for SPOT Level 1A and 1B stereo pairs (Valadan and Petrie, 1998) as well as, MOMS-O2 stereo images (Valadan, 1997) and IRS-1C stereo pairs (Valadan and Foomani, 1999).
The well known collinearity equation relates the points in the CT object coordinate system to the corresponding points in the image coordinate system. The relationship between these two coordinate systems is based on three rotations using combinations of the Keplerian elements mentioned above but computed with respect to the CT system using the transformation parameters between the CT and CI systems, plus three rotations, ω, φ, κ, for the additional undefined rotations of the satellite at the time of imaging. The off-nadir viewing angles of the linear array sensor must also be included as angle α and ß. The following equations will then result:

$$\begin{bmatrix} x_i - x_0 \\ y_i - y_0 \\ -c \end{bmatrix} = SR \begin{bmatrix} X_i - X_0 \\ Y_i - Y_0 \\ Z_i - Z_0 \end{bmatrix} \quad (5)$$

where

$$R = R_2(\alpha)R_1(\beta)R_3(\kappa)R_2(\varphi)R_1(\omega)R_2((f+\omega_p)-\pi/2)R_1(\pi/2-i)R_3(\Omega-\pi)$$

and

S :is the scale factor;

α,β :is the cross-track and along-track viewing angles;

x_i, y_i :are the image coordinates of object point *i*;

x_0, y_o :are the image coordinates of principal point;

X_i, Y_i, Z_i : are the object coordinates of image point *i*;

X_0, Y_0, Z_0: are the coordinates of the position of the sensor's perspective centre in the CT system;

c :is the principal distance ≈ focal length of the linear array imaging system, and

R_j :defines the rotation around the *j* axis, where j=1, 2 or 3.

Because of the dynamic geometry of linear array systems, the positional and attitude parameters of a linear array sensors are treated as being time dependent. The only available measures of time are the satellite's along-track coordinates. Thus the major components of the dynamic motion, the movement of the satellite in orbit and the Earth rotation are modelled as linear angular changes of *f* and Ω with respect to time, defined as f_1 and Ω_1. Thus:

$$f_i = f_0 + f_1 x,$$
$$\Omega_i = \Omega_0 + \Omega_1 x \qquad (6)$$

where,

f_i and Ω_i : are the true anomaly and the right ascension of the ascending node of each line i respectively;

f_0 and Ω_0 : are the true anomaly and the right ascension of the ascending node with respect to a reference line, for example the centre line of the scene; and

f_1 and Ω_1 : are the first values for the rates of change of f_i and Ω_i.

During the orientation of a pushbroom image, nine parameters of the orientation $(f_0, \Omega_0, a, i, f_1, \Omega_1, \omega_0, \varphi_0, \kappa_0)$ find the position in space of the satellite and its sensor system and its crude attitude. Considering the attitude of a scan line as a reference, the attitude parameters $\omega, \varphi,$ and κ of the other lines can therefore be modelled by a simple polynomial based on the along-track (x) image coordinates as follows:

$$\omega = \omega_0 + \omega_1 x + \omega_2 x^2$$
$$\varphi = \varphi_0 + \varphi_1 x + \varphi_2 x^2$$
$$\kappa = \kappa_0 + \kappa_1 x + \kappa_2 x^2 \qquad (7)$$

3.2.1. Orbital parameter modeling of Ikonos Geo image

The Keplerian elements $(f_0, \Omega_0, a, e, \omega_p)$,in-flight position ($X_0, Y_0, Z_0$) and viewing angle of the imaging sensor were approximated from meta data, image file, image acquisition geometry and celestial mechanics (Sadeghian, 2002).

A simpler and more pragmatic approach was implemented by the authors to convert Geo image to the corresponding raw image form. A comparison of the raw and Geo image shows one major difference in terms of geometry. As noted previously, the number of pixels per line in the raw image is 13500, while in this Geo image it is more than 13500. It is because off-nadir view angle of the image and the image has been rectified and resampled in such a way that each pixel has a pixel size of 1 m on the ground. With due attention to this difference, a procedure was devised and implemented by authors to carry out the required conversion.

The size of the Geo image (rectangle) is different from that of the corresponding raw image. Two coefficients are now computed to enable the final image to have the same size (13500 * 13500 pixels) in two directions as a raw image. These coefficients are used to produce the pixel and line coordinates of each point respectively from the following expressions:

Coefficient for the *p* coordinate = 13500/total number of pixels in each line

Coefficient for the *l* coordinate = 13500/total line of pixels in each scene

It will be seen that this procedure is somewhat akin to that of an affine transformation. However, additional displacements were introduced into the Geo imagery by the original corrections for each curvature/panoramic distortion. These displacements occur predominantly in the cross-track (y) direction and, since they are approximately symmetrical about the image center line, parameters adjusting the attitude as a function of the cross-track image coordinates should give a good correction for these displacements by replacing the terms in equation (3) by a term for this purpose, which leads to the following equations:

$$\omega = \omega_0 + \omega_1 x + \omega_2 y^2$$
$$\varphi = \varphi_0 + \varphi_1 x + \varphi_2 y^2$$
$$\kappa = \kappa_0 + \kappa_1 x + \kappa_2 y^2 \qquad (8)$$

Where x and y are the image coordinate. These equations have been incorporated in the procedure to transform the Geo image coordinates to their raw image form.

4. THE HAMEDAN IKONOS TESTFIELD AND IMAGE MENSURATION

The Ikonos Geo panchromatic image employed covered an 11 x 15 km area of central Hamedan city in the west of Iran (see Fig 1). It was acquired on 7 October 2000 with a 20.4º off-nadir angle and 47.4º sun elevations. Carterra Geo products are georectified, which means that they are rectified to an inflated ellipsoid and selected projection, in this case UTM on the WGS84 datum. No terrain-correction model is applied so these images are only rectified, as opposed to orthorectified. The stated accuracy of the Carterra Geo products is specified as 50 m CE90 exclusive of terrain displacement (Grodecki and Dail, 2001). In this investigation, the elevation within the Ikonos test area ranged from 1700 m to 1900 m. The GCPs/ICPs (Independent Check Points) for the tests were extracted from NCC-product digital maps, which employed a UTM projection on the WGS84 datum. In this instance the mapping scale was 1:1000 (see Fig. 2), with the compilation have been carried out using 1:4000 scale aerial photographs. The selected GCPs/ICPs in the imagery were distinct features such as building and pools corners, and wall and roads crossings, etc. The image coordinates of the GCPs/ICPs were monoscopically measured using the PCI EASI/PACE software system. These image measurements were then input into the least-squares adjustment computations, for the parameters of the DLT, SDLT and 3D affine as well as into the calculations for the orbital parameter model. The 1:1000 scale digital maps of Hamedan city were processed using commercially available software from PCI package for digital surface model (DSM) extraction. Figures 3 and 4 show some samples DSM of Hamedan.

Fig 1. Sample Ikonos Geo image of Hamedan, Iran

Fig 2. Sample 1:1000 scale map of Hamedan, Iran

Fig 3. Sample DSM of Hamedan, (Top view)

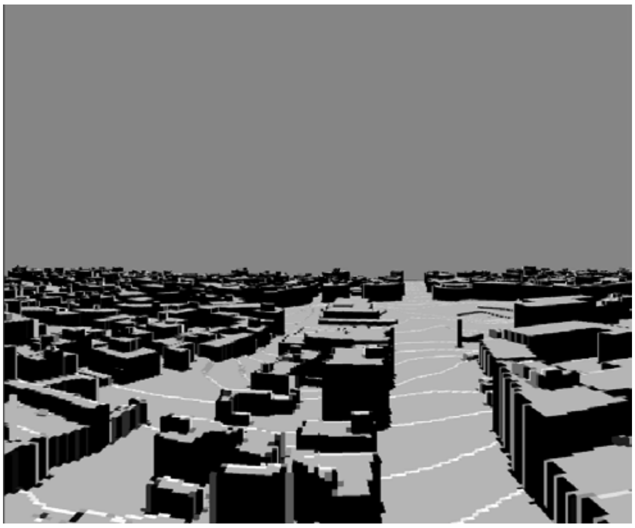

Fig 4. Sample DSM of Hamedan, (Front view)

5. PRACTICAL EVALUATION

DLT, SDLT and 3D Affine transformation computations were carried out with software written by the second author. Least squares determinations of the parameters of each orientation model were carried out using all available GCPs, namely 34 also 20 and 7 for the Ikonos image. The ground coordinates of ICPs were then determined utilizing the derived parameters and the differences between the photogrammetrically determined and map-recorded ground positions then formed the basis of the accuracy assessment phase. Table 1 shows summaries of the root mean square error (RMSE) obtained for the series of object point determinations, for the Ikonos image.Where ΔPl is represented as the square root of sum of ΔE and ΔN squares.

Table 1. ΔPl, RMSE values achieved in UTM coordinates of the Ikonos data over the Hamedan project area.

Method	GCPs Number	ICPs Number	Control Points ΔPl(m)	Check Points ΔPl(m)
3D Affine	34	20	1.02	0.97
	20	34	0.96	1.04
	7	47	0.91	1.10
DLT	34	20	0.95	0.95
	20	34	0.90	0.97
	7	47	0.59	1.90
SDLT	34	20	0.85	0.98
	20	34	0.82	0.96
	7	47	0.32	2.69

A bundle adjustment program implementing the mathematical model outlined in Part 3.2, written by the first author in Borland C++ for Windows and run on a PC, has been used to carry out the accuracy tests of the Ikonos Geo image. The bundle adjustment program is very flexible and the number of exterior orientation parameters can be reduced from 15 to 9 as a result of removing the quadratic and linear terms of the polynomials which model the change of the conventional rotation parameters (i.e. ω, φ and κ) with respect to time. The results of the bundle adjustment when using 9 combinations of control points and check points for the Hamedan test field are given in Table 2, 3, 4 and 5. The result of adjustment using equation (8) are stated in tables 5 and 6.

Table 2. ΔXY, residuals in WGS 1984 coordinates for the control and check points on the Ikonos Geo image corrected with 9 parameters and using equation 7, over the Hamedan project area.

GCPs Number	ICPs Number	Control Points	Check Points
		ΔXY(m)	ΔXY(m)
34	20	2.71	2.72
30	24	2.79	2.66
25	29	2.91	2.54
20	34	2.98	2.65
15	39	4.61	3.69
10	44	4.77	4.75
7	47	5.35	5.00
6	48	3.87	2.65
5	49	2.10	9.95

Table 3. ΔXY, residuals in WGS 1984 coordinates for the control and check points on the Ikonos Geo image with 12 parameters and using equation 7, over the Hamedan project area.

GCPs Number	ICPs Number	Control Points	Check Points
		ΔXY(m)	ΔXY(m)
34	20	2.43	2.48
30	24	2.49	2.35
25	29	2.57	2.29
20	34	2.61	2.42
15	39	3.97	3.28
10	44	3.88	4.29
7	47	3.88	4.71
6	48	3.12	2.53
5	49	0.14	15.36

Table 4. ΔXY, residuals in WGS 1984 coordinates for the control and check points on the Ikonos Geo image with 15 parameters and using equation 7, over the Hamedan project area.

GCPs Number	ICPs Number	Control Points	Check Points
		ΔXY(m)	ΔXY(m)
34	20	2.36	2.35
30	24	2.43	2.19
25	29	2.50	2.16
20	34	2.55	2.32
15	39	2.78	2.24
10	44	2.80	2.77
7	47	2.87	3.12
6	48	1.85	2.90
5	49	0.002	11.13

Table 5. ΔXY, residuals in WGS 1984 coordinates for the control and check points on the Ikonos Geo image with 15 parameters and using equation 8, over the Hamedan project area.

GCPs Number	ICPs Number	Control Points	Check Points
		ΔXY (m)	ΔXY (m)
34	20	1.01	1.31
30	24	1.00	1.26
25	29	1.06	1.19
20	34	1.15	1.10
15	39	1.67	1.45
10	44	1.33	2.16
7	47	0.97	2.13
6	48	0.35	2.83
5	49	0.00	13.76

As can be seen in Tables 4 and 5 using equation 8 yields better results than using equation 7. Also, the results show increased improvement for 15, 12 and 9 parameters equation respectively. However, from the practical test, equivalent RMSE values for independent check points in terms of the UTM coordinate system for 20 GCPs and 34 ICPs are given in table 6.

Table 6. R.m.s.e. values of the errors at the residual errors in the GCPs/ICPs in terms of both the WGS 1984 geocentric coordinate system and the UTM coordinate system on the Ikonos Geo image corrected with 15 parameters and using equation 8, over the Hamedan project area.

Method	Control Points (n=20)	Check Points (n=34)
	ΔPl (m)	ΔPl(m)
Orbital parameter	0.97	0.89

4. CONCLUSION

In this paper the accuracy potential of Ikonos Geo image was investigated. Rigorous models are not always available for satellite sensor orientation, especially for images from high resolution satellites such as Ikonos. Unlike the rigorous physical sensor model, non-rigorous models such as RFM, DLT, SDLT and 3D affine need no knowledge of the sensor model, or of orbit ephemeris and platform orientation parameters. Applications of these models to remotely sensed imagery acquired by Ikonos satellite indicate that relatively accurate geopositioning can be obtained through provision of ground control points.

High resolution data increase the need for higher accuracy of data modelling. In order to accurately model the imaging geometry of high resolution flexible pointing images such as Ikonos-2, EROSA-1, Quickbird-2, SPOT 5 and OrbView 3, we can use orbital parameter model. In this paper the flexibility and favourable accuracy of the orbital parameter model approach has been demonstrated with Ikonos Geo image and the method should be equally useful for other high resolution satellite imaging systems. This investigation has shown that Ikonos Geo imagery has high geometric integrity. When distinct object features such as building corners or roads crossings are used, an accuracy of better than 1 m can be achieved for Ikonos Geo with orbital parameter model. That accuracy is within the accuracy of Ikonos Precision Plus product.

Acknowledgements

The authors would like to acknowledge the Iranian Remote Sensing Center (IRSC) for providing the Ikonos image, and the National Cartographic Center (NCC) for providing 1:1000 scale digital maps of the test area.

References from Journals:

Dowman, I., and Tao C. V., 2002. An update on the use of rational functions for photogrammetric restitution, *Highlights ISPRS*, Vol. 7, No. 3, pp. 22-29.

Fraser, C.S., Baltsavias, E., Gruen, A., 2002a. Processing of Ikonos imagery for submeter 3D positioning and building extraction. ISPRS Journal of Photogrammetry & Remote Sensing, 56(2002), pp. 177-194.

Fraser, C.S., Hanley, H.B. and Yamakawa, T., 2002b. 3D geopositioning accuracy of Ikonos imagery, *Photogrammetric Record*, 17(99) , 465-479.

Gugan, D., 1986. Practical aspects of topographic mapping from SPOT imagery. *Photogrammetric Record*, 12(69), 349-355.

Hanley H.B. and Fraser C.S., 2001. Geopositioning accuracy of Ikonos imagery: indications from 2D transformations, *Photogrammetric Record*, 17(98), 317-329.

Radhadevi, P.V., Ramochandran, R. and Murali Mohan, A.S.R.K.V., 1998. Precision rectification of IRS-1C PAN data using an orbit attitude model. *ISPRS J. Photogrammetry and Remote Sensing*. 53(5), pp. 262-271.

Sadeghian, S., Valadan Zoej, M. J., Delavar and M. R., Abootalebi, A., 2001a. Precision rectification of KFA-1000 and IKONOS images using the multiquadric and DLT model over test areas in IRAN, *Photogrammetric Journal of Finland,* Vol. 17, No.2, pp.69-77.

Sadeghian, S., Valadan Zoej, M. J., Delavar and M. R., Abootalebi, A., 2001b. Precision rectification of high resolution satellite imagery without ephemeris data, *International Journal of Applied Earth Observation and Geoinformation (JAG),* Vol. 3, Issue 4, pp. 366-371.

Tao C. V. and Hu. Y., 2001. A comprehensive study of the rational function model for photogrammetric processing. *Photogrammetric Engineering and Remote Sensing,* 67(12):1347-1357.

Tao C. V. and Hu. Y., 2002. 3D Reconstruction methods based on the rational function model. *Photogrammetric Engineering and Remote Sensing,* 68(7):705-714.

Valadan Zoej, M. J. and Petrie, G., 1998. Mathematical modelling and accuracy testing of SPOT level 1B stereopairs. Photogrammetric Record, 16(91), pp. 67-82.

References from Other Literature:

Dowman, I. (Ed.), 1991. Test of triangulation of SPOT data. *OEEPE Publication,* No. 26, 206 pages.

Fraser C.S. and Shao, J., 1996. Exterior orientation determination of MOMS-O2 three-line imagery: experiences with the Australian testfield data. *Int'l Archives of Photogrammetry and Remote Sensing*, 31(Part B3): 207-214.

Gerlach, F.,2000. Characteristics of Space Imaging's one-meter resolution satellite imagery products. *Int'l Archives of Photogrammetry and Remote Sensing,* 33(Part B1): 128-135.

Grodecki, J. and Dial, G., 2001. Ikonos geometric accuracy, *Proceedings of Joint ISPRS Workshop on "High Resolution Mapping from Space 2001"* (CD ROM), 19-21 September, Hannover, Germany, unpaginated.

Sadeghian, S., 2002. Photogrammetric evaluation of high resolution space imagery for large scale mapping, Case study: Ikonos Geo pachromatic image of Iran. *PhD thesis, University of Tehran*:200 pages.

Sadeghian, S., Delavar M. R., 2003. An investigation of geometric correction and uncertainty assessment of high resolution images. *Second International Symposium on Spatial Data Quality*. Hong Kong, March, The Hong Kong Polytechnic University, pp. 89-99.

Valadan Zoej, M.J., Mansourian, A., Mojaradi, B. and Sadeghian, S., 2002. 2D geometric correction of Ikonos imagery using genetic algorithm, *Symposium on geospatial theory, processing and applications*, (CD-ROM), 9-12 July, Ottawa, unpaginated.

Valadan Zoej, M. J., 1997. Photogrammetric evaluation of space linear array imagery for medium scale topographic mapping. PhD thesis, volume1, University of Glasgow: 303 pages.

Valadan Zoej, M. J. and Foomani, J., 1999. Mathematical modeling and accuracy testing of IRS-1C stereo pairs. Joint Workshop of ISPRS WG I/1, I/3 and IV/4, Sensors and Mapping from Space, Hannover, September.

References from websites:

OGC (OpenGIS Consortium), 1999. *The OpenGIS Abstract Specification-Topic 7: The Earth Imagery Case*, URL: http://www.opengis.org/public/abstract/99-107.pdf.